Colloid Polym Sci (2006) 284: 1443–1451
DOI 10.1007/s00396-006-1523-6

ORIGINAL CONTRIBUTION

Daisuke Suzuki
Haruma Kawaguchi

Stimuli-sensitive core/shell template particles for immobilizing inorganic nanoparticles in the core

Received: 20 January 2006
Accepted: 7 March 2006
Published online: 29 June 2006

D. Suzuki · H. Kawaguchi (✉)
Faculty of Science & Technology,
Keio University,
3-14-1 Hiyoshi, Kohoku-ku,
Yokohama 223-8522, Japan
e-mail: haruma@applc.keio.ac.jp
Tel.: +81-45-5661563
Fax: +81-45-5645095

Abstract We synthesize and characterize stimuli-sensitive core/shell particles with functional group (or material) localized in the core. We previously reported two types of hybrid particles prepared by using the template particles which were synthesized by soap-free emulsion copolymerization with *N*-isopropylacrylamide and glycidyl methacrylate (GMA) as monomers but by different preparation methods. GMA has advantages in immobilizing materials having several functional groups such as thiol ones. In this study, to obtain the suitable template particles for immobilizing any inorganic nanoparticles in the core, we investigated the effect of feed ratio of the two monomers. Obtained template particles were modified by thiol compounds to introduce ionic groups. They were characterized by dynamic light scattering and scanning electron microscopy. After in situ synthesis of magnetic nanoparticles in the templates, the hybrid particles were characterized directly by transmission electron microscopy. Consequently, we could obtain the hybrid core/shell particles which contained a large amount of magnetic nanoparticles (~33 wt%) in the core.

Keywords Composite microgel particle · *N*-isopropylacrylamide · Glycidyl methacrylate · Inorganic nanoparticle · Core/shell particle

Introduction

Stimuli-sensitive particles based on poly(*N*-isopropylacrylamide) (PNIPAM) have received much attention due to their potential applications in biomedical [1] and optical [2] fields. PNIPAM particles which were monodisperse and of submicrometer were first synthesized via precipitation polymerization by Pelton and Chibante [3], and since then, numerous investigations about the preparation, characterization, and application were performed [4]. One of the important investigations is to design the structure and the distribution of functional groups for a specific application. Lyon's group reported specifically structured microgel particles such as core/shell and hollow ones [5, 6]. In their method, another shell layer, which had the same or different functional groups as those of core, was formed over the preformed microgel core. The core/shell microgel particles exhibited unique multiple-phase transition behavior with temperature [5]. They also synthesized hollow thermosensitive microgel particles by decomposing the microgel core selectively using periodate [6]. Hoare and Pelton [7] reported a series of PNIPAM-based microgel particles containing carboxylic acid groups prepared via copolymerization with vinylacetic acid, methacrylic acid, and acrylamide, which were selectively hydrolyzed to generate the carboxylic acid groups. They mentioned that functional groups are required to localize at a near surface of the particle for bioconjugation and medical diagnostics, whereas the particle interior is for control–release of drugs and dyes. The resultant three types of microgel particles had different distributions of carboxylic acids due to the different polymerization kinetics, relative hydrophobicity, and reaction pathway of the functional comonomers.

The objectives of this present study are to synthesize and characterize stimuli-sensitive core/shell particles with localizing functional group (or material) in the core using

NIPAM and glycidyl methacrylate (GMA) as monomers. We recently reported two types of hybrid particles. In the first case [8a], Au nanoparticles were attached in the thermosensitive hydrogel phase of the template particle. The hybrid particles could exhibit reversible color change due to interparticle interactions of the nanoparticles by temperature change. In that case, the Au nanoparticles were required to be attached and dispersed independently in thermosensitive hydrogel phase to clarify the color change. In the second case [8b], the Au nanoparticles were localized around the rigid core surface which was covered with thermosensitive shell composed of PNIPAM. In that case, the core/shell structure of the template was necessary to obtain the hierarchal organic/inorganic sphere. In those two cases, we used the template particles synthesized by soap-free emulsion copolymerization with NIPAM and GMA as monomers but by different preparation methods. GMA has advantages in immobilizing materials having several functional groups such as the thiol ones. We observed that almost all Au nanoparticles were in situ synthesized at the point where functional group existed. In general, taking the reactive ratios and hydrophilicity of the two monomers into account, particles with PGMA-rich core and PNIPAM-rich shell are expected to be obtained. In this study, to obtain the suitable core/shell template particles for immobilizing inorganic nanoparticles in the core, we investigated the effect of feed ratio of the two monomers. Obtained template particles were modified by thiol compounds to introduce ionic groups. They were characterized by dynamic light scattering (DLS) and scanning electron microscopy (SEM). After in situ synthesis of inorganic nanoparticles in the template particles, the hybrid particles were characterized directly by transmission electron microscopy (TEM). Consequently, we could obtain the hybrid core/shell particles which contained a large amount of magnetic nanoparticles (~33 wt%) in the core.

Experimental section

Materials

Unless stated otherwise, all materials were purchased from Wako Pure Chemical Industries. NIPAM was kindly given by Kojin and recrystallized from hexane–toluene (1:1 on a volume basis). GMA was purified by distillation under a reduced pressure to remove inhibitors. *N*,*N*′-methylenebis acrylamide (MBAAm) was used without further purification. Azobisamidinopropane dihydrochloride (V-50) was used without further purification. 3-Mercapto-1-propane sulfonic acid sodium salt (MPSA, Aldrich), 2-aminoethanethiol (AET, Tokyo Kasei Kogyo), and mercaptoacetic acid (MAA) were used without further purification. Sodium nitrate ($NaNO_2$), iron sulfate ($FeSO_4$ $7H_2O$, Junsei Chemical), and ammonia solution (28% NH_4OH, Junsei Chemical) were used as received. The water used in all experiments was from a Milli-Q reagent water system (Millipore).

Preparation and functionalization of NIPAM-*co*-GMA (NG) template particles

To obtain the templates, NIPAM, GMA, and MBAAm were copolymerized with different feed ratios in a soap-free aqueous medium using V-50 as an initiator, subsequently modified with thiol compounds. In this study, to obtain the best candidate template for localizing various inorganic nanoparticles in the core, several templates were prepared. A mixture of NIPAM (1.0–3.0 g), GMA (0–2.0 g), MBAAm (0.04 g), and water (90 g) was poured into a 200-ml, three-necked round-bottom flask equipped with a stirrer, a nitrogen gas inlet, and a condenser. Nitrogen gas was bubbled into the mixture to purge oxygen. The mixture was kept at 70 °C in an oil bath. V-50 initiator (0.06 g) was dissolved in water (10 g) and added to the flask for the initiation of the polymerization, which then continued for 6 h. The obtained particles (NG particles) were purified by centrifugation, decantation, and then washed with water. This purification cycle was carried out four times.

Then, the epoxy groups in NG template particles were allowed to react with thiol groups of MPSA, AET, and MAA to introduce the functional groups to the particles. A mixture of NG particles (1.0 g), thiol compounds (ten times amount against epoxy groups in each microgel), and water (90 g) was poured into a 100-ml glass vial with stirring under room temperature, and the pH was adjusted to 11 with 6 N NaOH. The reaction was continued for 24 h. The obtained template particles (NG–MPSA, NG–AET, and NG–MAA) were purified by the same method described above, and by 1 week of dialysis, in addition.

In situ synthesis of magnetic nanoparticles in the template particles

In situ synthesis of magnetic nanoparticles was performed according to the modified method described previously [9]. A mixture of the NG–MPSA template particles (0.3 g), $FeSO_4$ $7H_2O$ (1.2 g), and water (20 ml, prepurged with N_2, pH 3) was put into a 30-ml glass vial under room temperature, and it was agitated for 4 h. After removing excess ions by centrifugation, the dispersion (total volume was 20 ml) was put into a 50-ml, three-necked round-bottom flask equipped with a stirrer, a nitrogen gas inlet, and a condenser. Nitrogen gas was bubbled into the mixture for 1 h to purge oxygen. After that, a 1-ml aqueous solution of $NaNO_2$ (18 mg) was added to the flask. After 15 min, a 2.4 ml of 28% ammonia solution was injected into the flask. After 2 h, the hybrid particles (NG–MPSA–

Mag) were purified by centrifugation which was the same method described above.

Characterization

Approximately 2 μl of the diluted particle suspension was dried on carbon-coated copper grids and observed by field emission TEM (TECNAI F20, Philips Electron Optics) operated at 200 kV. Also, approximately 5 μl of the diluted particle suspension was dried on a polystyrene substrate and observed by field emission SEM (S-4700, Hitachi). The SEM samples were sputter-coated with platinum/palladium before examination. Hydrodynamic diameters of particles were determined by DLS using a laser particle analyzer system (PAR-3, Otsuka Electronic). The incident wavelength was 632 nm of a He–Ne laser, and the measurement angle was 90 °. The samples for DLS experiment were allowed to equilibrate at each temperature for 10 min before measurements. An elemental analysis of dried samples for carbon, hydrogen, nitrogen, oxygen, and sulfur was conducted by Vario EL (Elementar Analysensysteme GmbH). The magnetic nanoparticle content of the dried samples was measured by thermogravimetry. The thermogravimetric analysis (TGA) measurements were performed with a Seiko instrument, the TG-DTA 6200. The temperature range was between 30 and 600 °C with a heating rate of 20 K min^{-1}.

Results and discussions

As shown in Scheme 1, our objectives in this study are to characterize functional group distribution of the template particles and to obtain the hybrid core/shell particles which localize magnetic nanoparticles in the core. NG particles were prepared by soap-free emulsion copolymerization of NIPAM and GMA with different feed ratios using MBAAm as a cross-linker. Because of the different reactivity ratios of NIPAM and GMA (0.39 and 2.69, respectively) [10], GMA tended to be consumed faster than NIPAM. In addition, each polymer's hydrophilicity was not very different at 70 °C; the most outer layer of each NG particle was supposed to be rich in PNIPAM regardless of

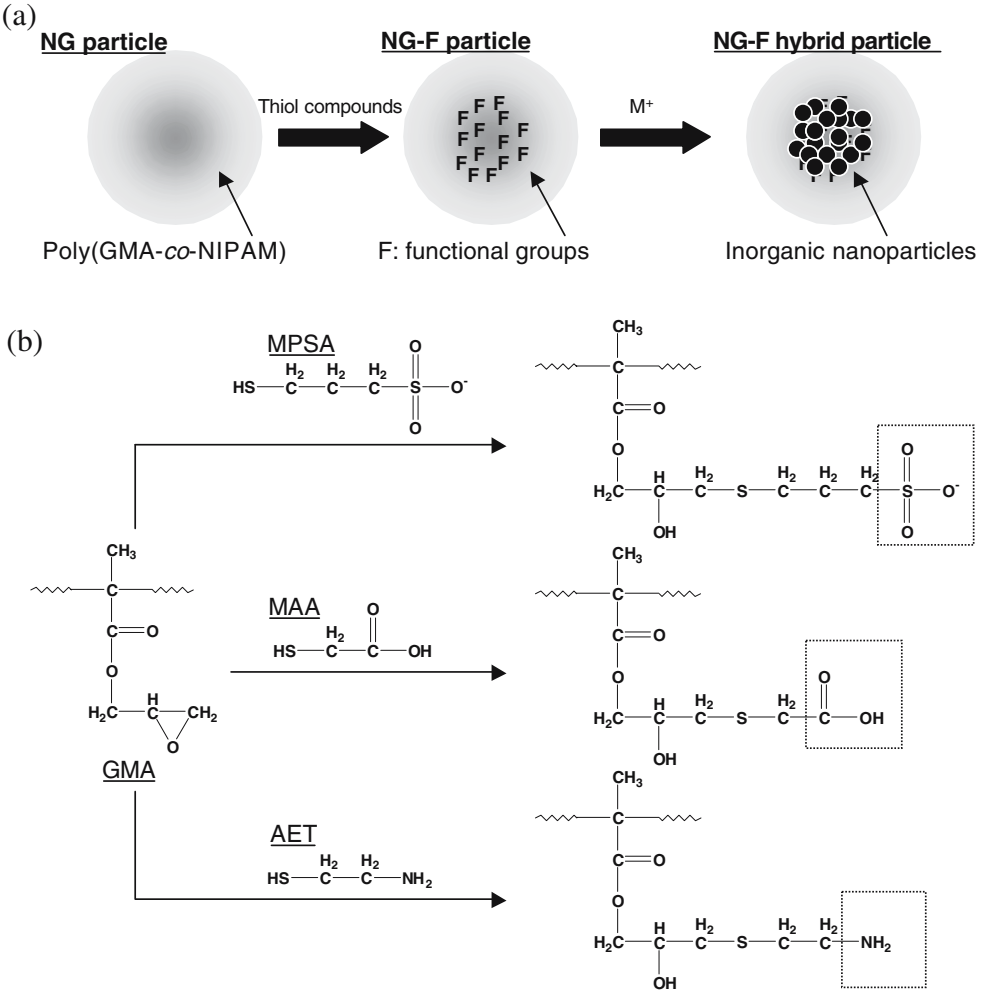

Scheme 1 Preparation of the hybrid particle (**a**), and introduction method of functional groups to the particle (**b**)

monomer feed ratio although cross-linking inhomogeneity must exist [11]. If a core/shell template in which core has the space for generation of inorganic nanoparticles and affinity with their precursor ions, whereas shell has only thermosensitivity, the nanoparticles will be synthesized in situ only in the core. GMA can be modified to introduce functional groups of materials such as proteins. In this study, MPSA, AET, and MAA were introduced, respectively, as shown in Scheme 1b.

Preparation and characterization of the template particles

Under any conditions in this study, monodisperse NG particles were obtained, which was confirmed by DLS measurement. Figure 1 shows the temperature dependence of the hydrodynamic diameters of the NG and MPSA incorporated (NG–MPSA) particles in aqueous dispersion measured by DLS. The sample code and monomer feed ratios of NG particles are summarized in Table 1. It should

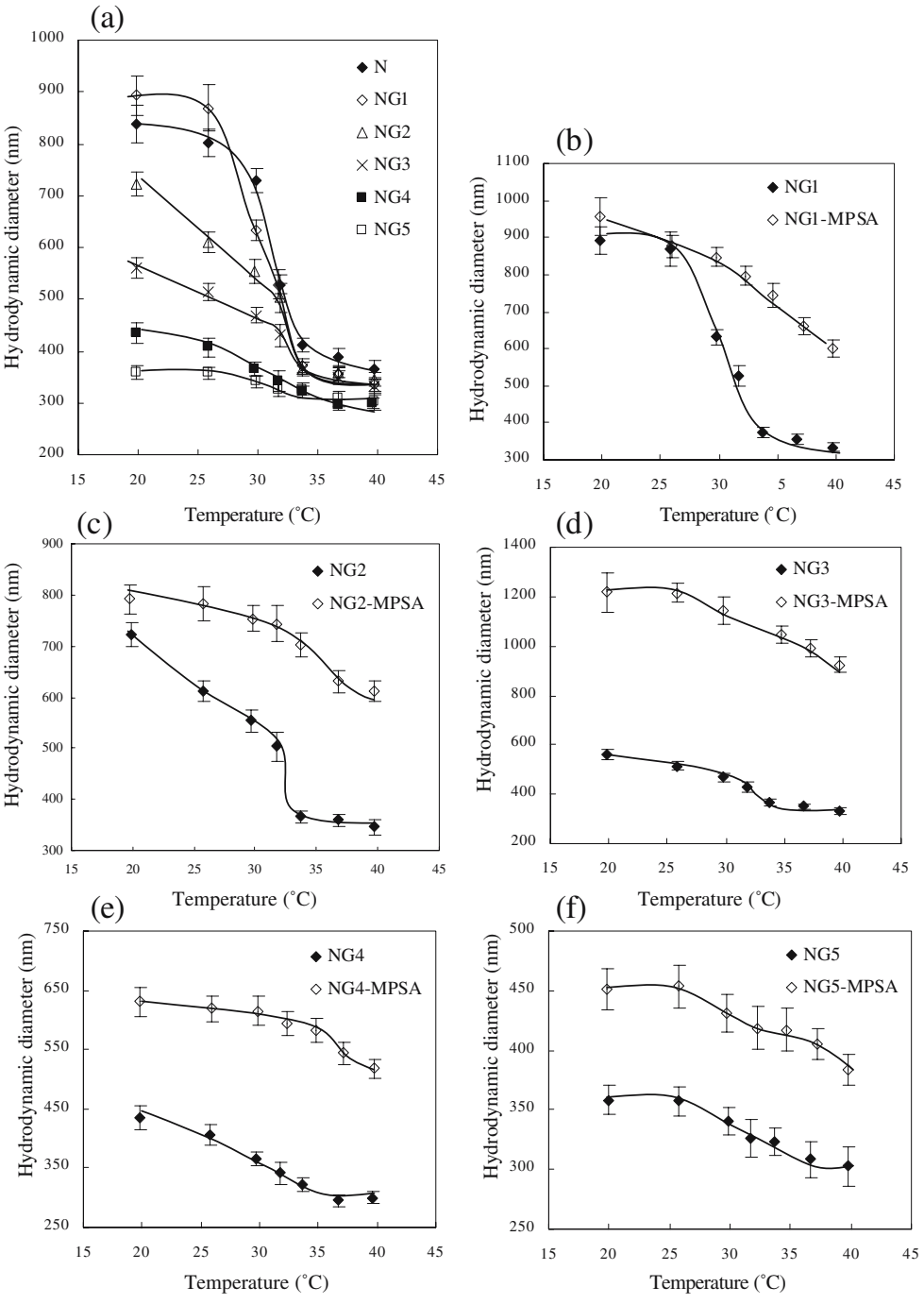

Fig. 1 Temperature dependence of the hydrodynamic weight-averaged diameter in aqueous dispersions (pH 6) measured by dynamic light scattering (temperature-raising process). **a** N (♦) and a variety of NG [NG1 (◊), NG2 (Δ), NG3 (×), NG4 (¦), NG5 (?)] particles. **b** NG1 (♦) and NG1–MPSA (◊) particles. **c** NG2 (♦) and NG2–MPSA (◊) particles. **d** NG3 (♦) and NG3–MPSA (◊) particles. **e** NG4 (♦) and NG4–MPSA (◊) particles. **f** NG5 (♦) and NG5–MPSA (◊) particles

Table 1 Preparation conditions, weight-averaged hydrodynamic diameters (D_w) and swelling ratios (V/V_0) of N and a variety of NG particles

Code	NIPAM mass (g)	GMA mass (g)	D_w at 20 °C (nm)	D_w at 40 °C (nm)	D_w at 70 °C (nm)	V/V_0[a] at 40 °C (−)	V/V_0 at 70 °C (−)
N	3.0	0	838	365	354	0.083	0.075
NG1	2.8	0.2	893	334	308	0.052	0.041
NG2	2.5	0.5	723	346	328	0.110	0.093
NG3	2.0	1.0	560	331	309	0.206	0.168
NG4	1.5	1.5	435	296	273	0.315	0.247
NG5	1.0	2.0	358	303	276	0.606	0.458

[a] V_0 is a volume of each NG particle at 20 °C

be mentioned that the DLS measurement was performed only at 90 °, and consequently, the obtained hydrodynamic diameters shown in this study are not highly accurate. However, the comparison of DLS data is still meaningful for the analysis of thermosensitive properties. In all data shown in Fig. 1, the dispersion contained no salt, and the pH value was not adjusted. The pH was around 6. The dispersity, the ratio of the weight-averaged diameter to the number-averaged diameter, was less than 1.04 in all cases. The diameter of NG particles at the swollen state decreased as GMA feed ratio increased, whereas those were nearly the same (~300 nm) at the deswollen state (Fig. 1a). All of the NG particles exhibited the volume phase transition of PNIPAM around ~33 °C, but the response became duller as GMA feed ratio increased. This may be because not only the inhomogeneously cross-linked network structure restricted the chain motion and retarded the response [12] but also the gradient distribution of GMA in the particles due to the different values of reactive ratio. GMA made the polymer chains hydrophobic, which made them shrunken even at lower temperature than that of pure PNIPAM microgels [13]. Although these data reveal that all NG particles showed thermosensitivity, the core/shell structures we speculated are still unclear.

Next, functional groups were introduced to each NG particle using thiol compounds (see Scheme 1b). First, we investigated the hydrodynamic diameters of the sulfonated particles (NG–MPSA) to diminish the effect of pH on the functional groups. The amount of introduced functional groups was calculated from sulfur content measured by elemental analysis. Table 2 shows the sample codes and the number of their sulfonate groups per particle. In all cases, the hydrodynamic diameters at 20 °C increased after MPSA introduced, and even at 40 °C, they had not reached their fully deswollen states yet due to electrostatic repulsion among sulfonate groups (Fig. 1b–f) [14]. Tables 1 and 2 also show the swelling ratios defined as follows: V/V_0, the volume of particles at 20, 40, and 70 °C were divided by the volume of (their parent) NG particles at 20 °C. It should be noted that the volume of NG3–MPSA particle became ten times larger than that of NG3 particle at 20 °C while the swelling ratios of the other sulfonated particles were not very high values. Even though the amount of introduced sulfonate groups was not very different between NG2– and NG3–MPSA, the swelling ratios were much different between them due to the structure difference between their parent particles. For NG1– and NG2–MPSA particles, the relatively lower swelling ratios than that of NG3–MPSA particle were because NG1 and NG2 particles had already reached their highly swollen states at 20 °C but the NG3 particle had not. On the other hand, the swelling ratios of NG4– and NG5–MPSA were smaller than that of NG3–MPSA although the sulfonate groups introduced were not very different. These data indicate that MPSA could not permeate into the core of NG4 and NG5 microgels or could permeate into there but the resultant particles could not swell because of high cross-linking and strong hydropho-

Table 2 The number of immobilized sulfonate groups to a variety of nG particles, weight-averaged hydrodynamic diameters (D_w) and swelling ratios (V/V_0) of a variety of NG–MPSA particles

Code	Parent particle	Sulfonate group[a] (number/particle)	D_w at 20 °C (nm)	D_w at 40 °C (nm)	D_w at 70 °C (nm)	V/V_0[b] at 20 °C (−)	V/V_0 at 40 °C (−)	V/V_0 at 70 °C (−)
NG1–MPSA	NG1	1.5×10^5	957	634	393	1.231	0.358	0.085
NG2–MPSA	NG2	5.8×10^6	792	611	471	1.315	0.604	0.276
NG3–MPSA	NG3	1.0×10^7	1217	925	769	10.264	4.507	2.589
NG4–MPSA	NG4	6.4×10^6	631	543	380	3.052	1.945	0.667
NG5–MPSA	NG5	4.9×10^6	432	418	347	1.757	1.592	0.911

[a] Calculated from elemental analysis data
[b] V_0 is a volume of each parent NG particle at 20 °C

bic interactions among PGMA chain segments. Taking all things into consideration, NG3 particle seemed to localize a large amount of sulfonate groups in the core, and the resultant particles swelled much more than the parent particle. In other words, functional group-immobilized NG3 particle has the potential to be the best candidate for synthesizing inorganic nanoparticles in the core among all microgels shown in this investigation.

In addition, temperature dependence of the hydrodynamic weight-averaged diameter of AET- and MAA-immobilized NG3 particles (NG3–AET and NG3–MAA, respectively) in different pH solutions was investigated for confirming the utility of NG3 particle (Fig. 2). Although the number of introduced AET or MAA (3.8×10^6 and 3.9×10^6 U/particle, respectively) and the swelling ratios at 20 °C (7.108 and 7.112, respectively), which were defined in this investigation above, of NG3–AET and NG3–MAA particles are a bit smaller than that of NG3–MPSA, the temperature dependences of them at pH 9 for NG3–AET and at pH 3 for NG3–MAA nearly corresponded to that of NG3 particle. This fact suggests that NG3 particle can be modified by any thiol compounds at room temperature.

Figure 3 shows SEM views of several NG particles dried on the polystyrene substrate at room temperature. Each particle spontaneously arranged with spaces on the polystyrene substrate due to the unique property of PNIPAM-covered particles [3, 15]. The particles composing of mainly PNIPAM (samples of N, NG1, NG2, and NG3) were settled down, retaining their own excluded volume, and were regularly arranged on the substrates. These dried particles were deformed due to water evaporation from the hydrogel phase. On the other hand, in the case of the PGMA-rich particles (sample of NG5), although the particle arrangement was disturbed due to less excluded volume of PNIPAM shell, they were also settled down with spaces. The dried structure of NG5 particle was not very deformed like the other particles. These data suggest that NG5 has a rigid core composed of mainly PGMA and PNIPAM shell.

After immobilizing MPSA to the particles, the degree of the particle deformation at a dried state increased due to higher swelling ratio than that of the parent particle, especially for NG3–MPSA (Fig. 4), but the particles were ordered as like the parent particles. These data support previous report of our group [15] that electrical interaction between particles did not have a large effect on ordering, but swelling ratio affected the degree of structure deformation at a dried state.

In situ synthesis of magnetic nanoparticles using microgel templates

We conducted further investigations about in situ synthesis of magnetic nanoparticles using several template particles characterized above. Magnetic nanoparticles were synthesized by coprecipitation method reported previously [9, 16]. Figure 5 presents TEM views of five types of the hybrid magnetic particles. We found from TEM views that the magnetic nanoparticles were formed only in the template particles except NG5–MPSA–Mag particles, which (the formation) was also confirmed by DLS analysis.

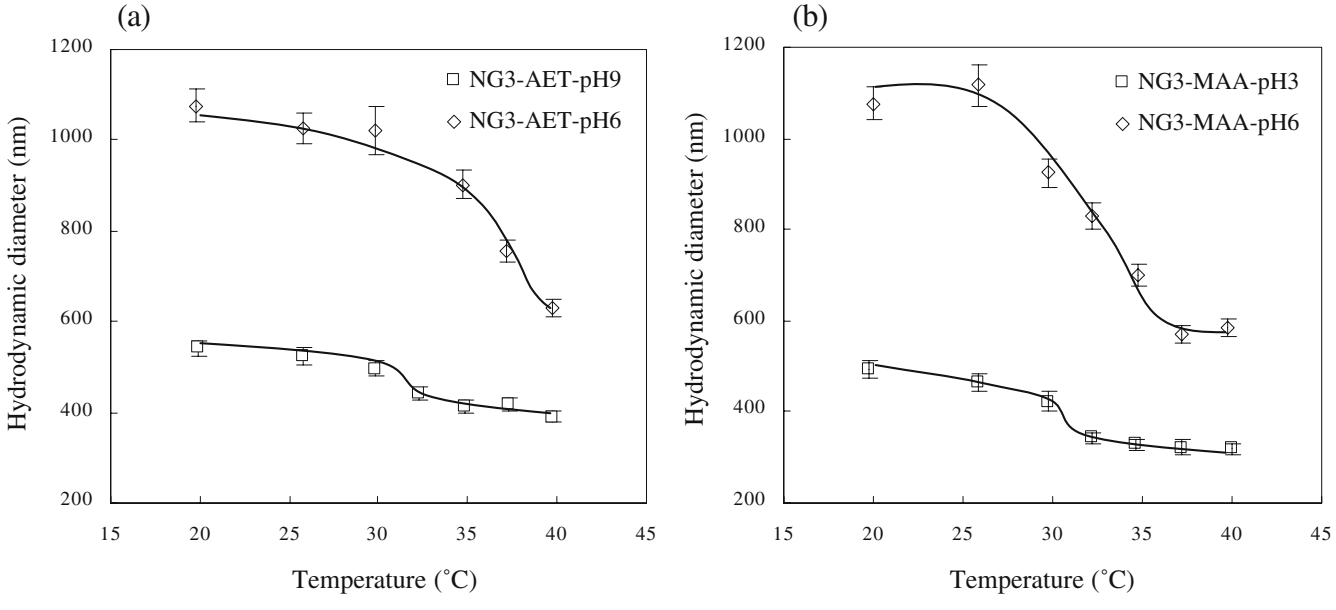

Fig. 2 Temperature dependence of the hydrodynamic weight-averaged diameters in aqueous dispersions measured by dynamic light scattering (temperature-raising process). **a** NG3–AET particles at pH 9 (?) and at pH 6 (◊). **b** NG3–MAA particles at pH 3 (?) and at pH 6(◊)

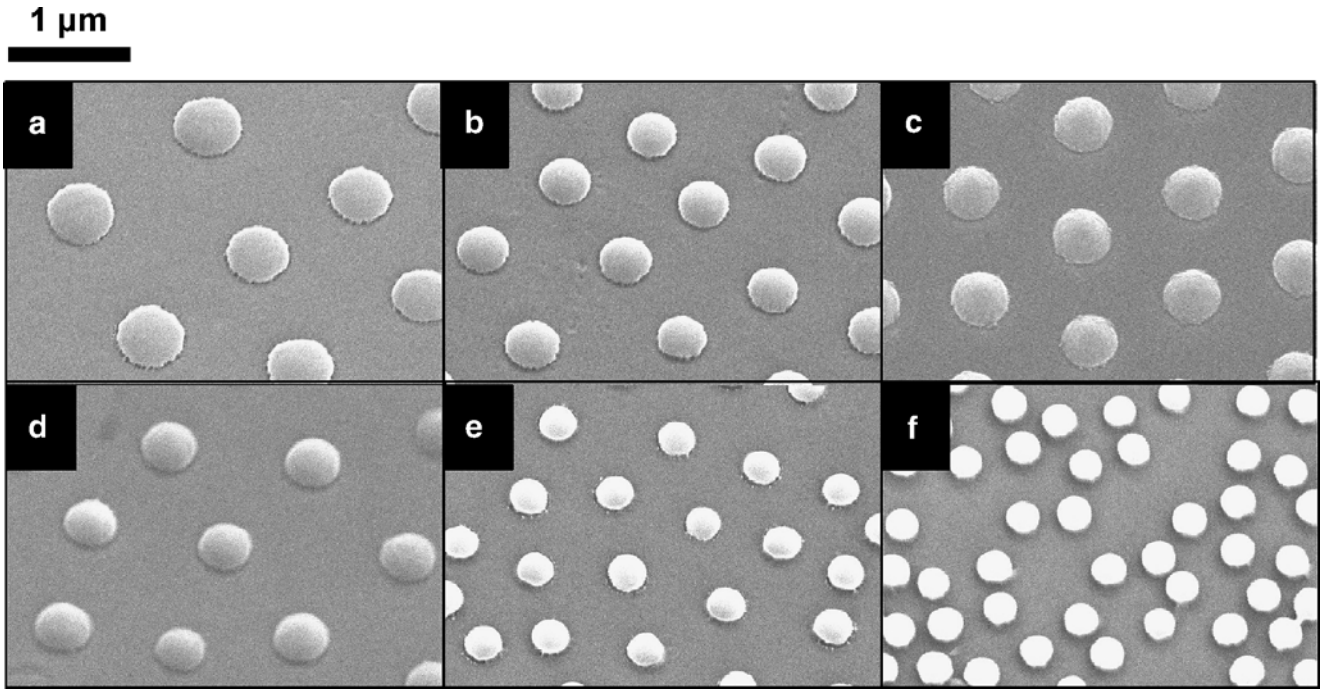

Fig. 3 SEM views of several NG particles on the polystyrene substrate dried at room temperature. **a** N, **b** NG1, **c** NG2, **d** NG3, **e** NG4, and **f** NG5 particles. *Each picture* was taken at the same magnification

The almost same average diameters (~13 nm) from TEM views were obtained for NG1–, NG2–, NG3–, and NG4–MPSA–Mag particles although that of NG5–MPSA–Mag particle was ~66 nm. This difference of NG5–MPSA–Mag particle might be due to less effect of polymer chain networks for generating nanoparticles [8, 16].

TGA measurements revealed that each magnetic nanoparticle content was 11.1, 16.0, 32.9, 10.1, and 6.2 wt% for NG1–MPSA–Mag to NG5–MPSA–Mag particles, respectively. The highest value of magnetic nanoparticle content was obtained from NG3–MPSA–Mag particles. This was due to the template structure and composition. Taking reactive ratios of NIPAM and GMA into consideration, the core/shell structure in which core has the space for generating magnetic nanoparticles and localizes sulfonate groups attaching precursor iron ions—whereas only shell has thermosensitivity—should be formed. But, we assumed, such structure is formed effectively only when monomer feed ratio is well balanced. Compared to NG2–MPSA and NG4–MPSA template particles, NG3–MPSA particle was the best candidate template that satisfied above-mentioned requirement and can localize large amounts of inorganic nanoparticles.

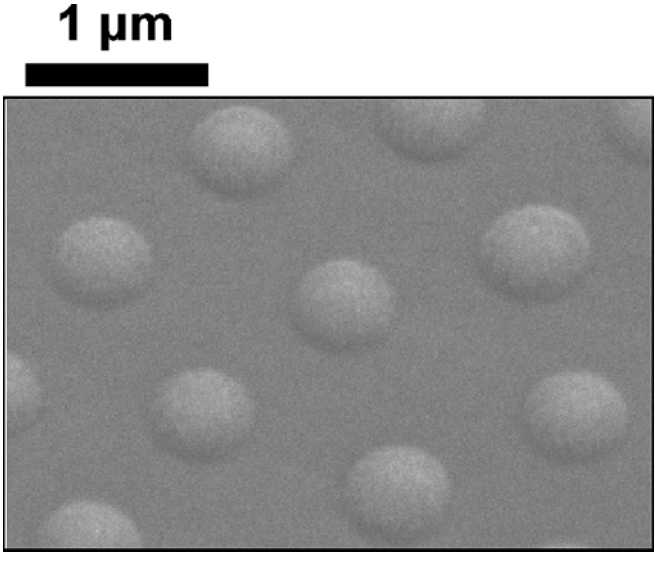

Fig. 4 SEM view of NG3–MPSA particles on the polystyrene substrate dried at room temperature

The hybrid core/shell particles have potential magnetic and biomedical applications. Because all magnetic nanoparticles are localized in the core, the outer shell layer prevents the hybrid particle from aggregation. For example, construction of particle chain or labyrinthic structures would be tuned by external stimuli such as pH and temperature as well as an external magnetic field without leaking magnetite and aggregating the hybrid particles [17, 18]. In addition, high amounts of magnetite-encapsulated particles would be used as magnetic drug targeting [19] and chemical separation [20]. Furthermore, other inorganic nanoparticles such as Au [8], Ag [16, 21], and semiconductor ones [16, 22] would also be synthesized easily in cationic or anionic core/shell particles shown in

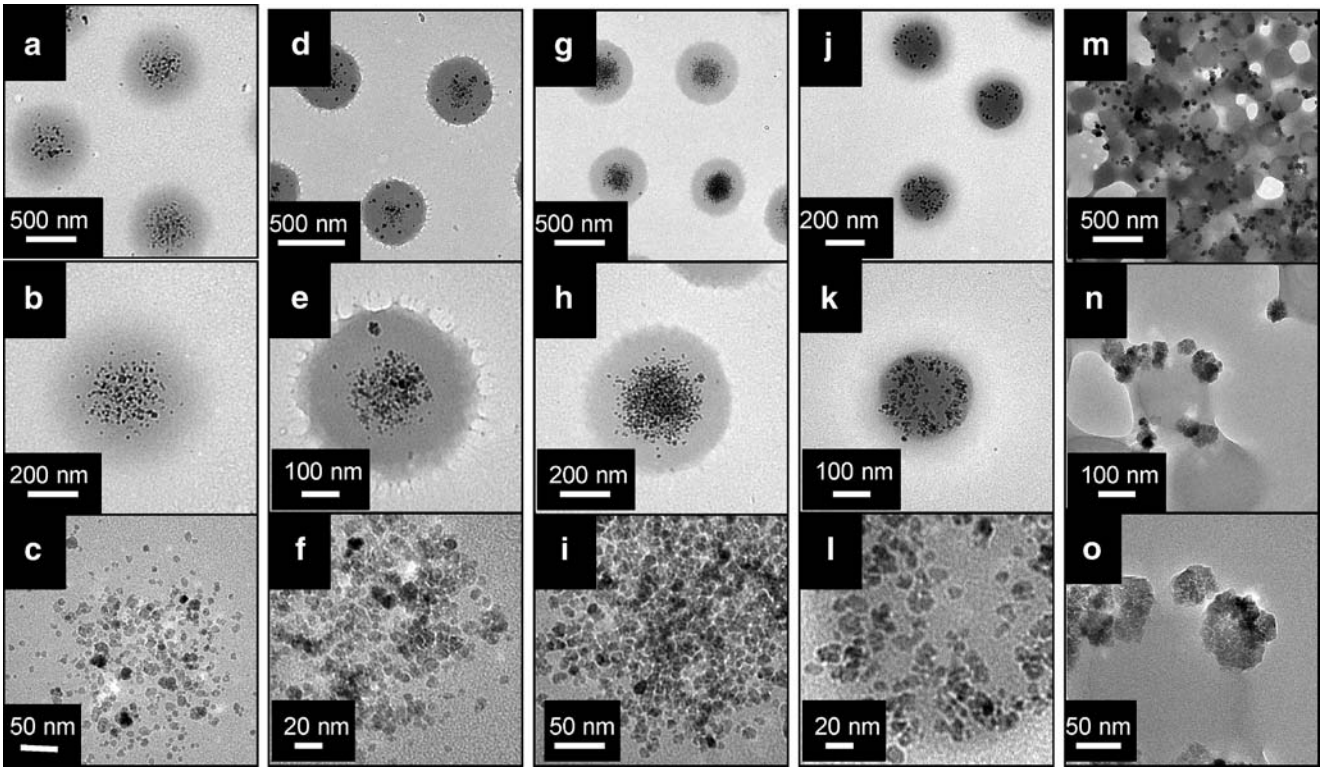

Fig. 5 TEM views of the hybrid particles deposited on carbon-coated copper grid dried at room temperature. Hybrid particles using NG1–MPSA (**a**, **b**, **c**), NG2–MPSA (**d**, **e**, **f**), NG3–MPSA (**g**, **h**, **i**), NG4–MPSA (**j**, **k**, **l**), and NG5–MPSA (**m**, **n**, **o**) particles as templates. *Each triplet* was taken at different magnifications

this present study, and the hybrid core/shell particles also have potential optical and electrical applications.

Conclusions

We synthesized stimuli-sensitive core/shell template particles with functional group localized in the core for immobilizing inorganic nanoparticles using NIPAM and GMA as monomers. NG template particles could be modified by thiol compounds to introduce ionic groups such as amino, carboxyl, and sulfonate groups. A series of the template particles were characterized by DLS and SEM. After in situ synthesis of magnetic nanoparticles in the particles, the hybrid particles were characterized directly by TEM. The well-balanced monomer feed ratio for obtaining the best template particles existed, and consequently, we could obtain the hybrid core/shell particle which contained a large amount of magnetic nanoparticles (~33 wt%) in the core. The hybrid core/shell particles synthesized with reflecting predetermined template structures have potential magnetic and biomedical applications as well as optical and electrical ones.

Acknowledgements D. S. thanks the research fellowships of the Japan Society for the Promotion of Science for Young Scientists. This work was supported by a Grant-in-Aid for the 21st Century COE program "KEIO Life-Conjugated Chemistry" from the Ministry of Education, Culture, Sports, Science, and Technology, Japan.

References

1. (a) Kawaguchi H, Fujimoto K, Mizuhara Y (1992) Colloid Polym Sci 270:53. (b) Topp MDC, Dijkstra PJ, Talsma H, Feijen J (1997) Macromolecules 30:8518
2. (a) Weissman JM, Sunkara HB, Tse AS, Asher SA (1996) Science 274:959. (b) Holtz JH, Asher SA (1997) Nature 389:829. (c) Gao J, Hu Z (2002) Langmuir 18:1360. (d) Jones CD, Lyon LA (2003) J Am Chem Soc 125:460
3. Pelton RH, Chibante P (1986) Colloids Surf 20:247
4. Pelton R (2000) Adv Colloid Interface Sci 85:1

5. (a) Jones CD, Lyon LA (2000) Macromolecules 33:8301. (b) Gan D, Lyon LA (2001) J Am Chem Soc 123:7511. (c) Gan D, Lyon LA (2001) J Am Chem Soc 123:8203. (d) Jones CD, Lyon LA (2003) Macromolecules 36:1988
6. Nayak S, Gan D, Serpe MJ, Lyon LA (2005) Small 4:416
7. (a) Hoare T, Pelton R (2004) Langmuir 20:2123. (b) Hoare T, Pelton R (2004) Macromolecules 37:2544
8. (a) Suzuki D, Kawaguchi H (2005) Langmuir 21:8175. (b) Suzuki D, Kawaguchi H (2005) Langmuir 21:12016
9. (a) Shinkai M, Honda H, Kobayashi T (1991) Biocatalysis 5:61. (b) Kondo A, Kamura H, Higashitani K (1994) Appl Microbiol Biotechnol 41:99
10. Virtanen J, Tenhu H (2001) J Polym Sci Part A Polym Chem 39:3716
11. Wu X, Pelton RH, Hamielec AE, Woods DR, McPhee W (1994) Colloid Polym Sci 272:467
12. (a) Ohshima H, Makino K, Kato T, Fujimoto K, Kondo T, Kawaguchi H (1993) J Colloid Interface Sci 159:512. (b) Kato T, Fujimoto K, Kawaguchi H (1994) Polym Gels Netw 4:307
13. Gao J, Frisken BJ (2005) Langmuir 21:545
14. García-Salinas MJ, Romero-Cano MS, de las Nieves FJ (2001) J Colloid Interface Sci 241:280
15. (a) Tsuji S, Kawaguchi H (2004) Langmuir 20:2449. (b) Tsuji S, Kawaguchi H (2005) Langmuir 21:2434. (c) Tsuji S, Kawaguchi H (2005) Langmuir 21:8139
16. Zhang J, Xu S, Kumacheva E (2004) J Am Chem Soc 126:7908
17. Skjeltorp AT (1983) Phys Rev Lett 51:2306
18. Wang H, Zhu Y, Boyd C, Luo W, Cebers A, Rosensweig RE (1994) Phys Rev Lett 72:1929
19. (a) Lubbe AS, Bergemann C, Huhnt W, Fricke T, Riess H, Brock JW, Huhn D (1996) Cancer Res 56:4694. (b) Viroonchatapan E, Ueno M, Sato H, Adachi I, Nagae H, Tazawa K, Horikoshi I (1995) Pharm Res 12:1176
20. Kawaguchi H, Fujimoto K (1998) Bioseparation 7:253
21. Zhang J, Xu S, Kumacheva E (2005) Adv Mater 17:2336
22. Pich A, Hain J, Lu Y, Boyko V, Prots Y, Adler H-J (2005) Macromolecules 38:6610